

Space-Vector PWM Inverter Feeding a Permanent-Magnet Synchronous Motor

A. Maamoun, Y. M. Alsayed, and A. Shaltout

Abstract—The paper presents a space-vector pulse width modulation (SVPWM) inverter feeding a permanent-magnet synchronous motor (PMSM). The SVPWM inverter enables to feed the motor with a higher voltage with low harmonic distortions than the conventional sinusoidal PWM inverter. The control strategy of the inverter is the voltage / frequency control method, which is based on the space-vector modulation technique. The proposed PMSM drive system involving the field-oriented control scheme not only decouples the torque and flux which provides faster response but also makes the control task easy. The performance of the proposed drive is simulated. The advantages of the proposed drive are confirmed by the simulation results.

Keywords—permanent-magnet synchronous motor, space-vector PWM inverter, voltage/frequency control.

I. INTRODUCTION

THE space-vector pulse width modulation (SVPWM) technique has become a popular pulse width modulation technique for three-phase voltage-source inverter in the control of AC motors [1]-[3]. Among the various types of AC motors, the permanent-magnet synchronous motor (PMSM) is becoming a very popular choice in drive technology due to some of its inherent advantageous features. These features include high torque to current ratio, large power to weight ratio, higher efficiency, and robustness. The PMSM drive system involving the field-oriented control scheme not only decouples the torque and flux which provides faster response but also makes the control task easy [4]-[7].

The SVPWM voltage-source inverters for variable voltage variable frequency (VVVF) drives of PMSM are widely used in both industrial and household applications. The SVPWM inverter is used to offer 15% increase in the dc-link voltage utilization and low output harmonic distortions compared with the conventional sinusoidal PWM inverter. The control strategy of the inverter is the voltage/frequency control method, which is based on the space-vector modulation technique. The SVPWM inverter enables to feed the motor with a higher voltage with low harmonic distortions than the conventional PWM inverter. The SVPWM allows to having a higher torque at high speeds, and a higher efficiency.

In this paper the SVPWM inverter which feeding a PMSM is simulated by using the Matlab software package. The simulation is performed for PMSM of 0.95 kW. The performance of the proposed model of the SVPWM inverter feeding a PMSM is simulated at different loading conditions. The advantages of the proposed drive are confirmed by the simulation results.

II. SVPWM TECHNIQUE

The power circuit of a three-phase voltage-source inverter (VSI) is shown in Fig. 1, where V_a , V_b , and V_c are the output voltages applied to the star-connected motor windings, and where V_{dc} is the continuous inverter input voltage. S_1 through S_6 are the six power transistors those shape the output, which are controlled by switching signals. When an upper transistor is switched on, the corresponding lower transistor is switched off. There are eight different combinations of switching states as follows : (000), (100), (110), (010), (011), (001), (101), and (111). The first and last states do not cause a current to flow to the motor, and hence, the line-to-line voltages are zero. The other six states can produce voltages to be applied to the motor

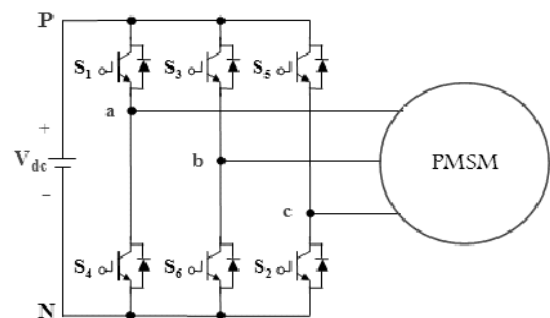


Fig. 1 Three-phase VSI bridge circuit

A. Maamoun is with the Electronics Research Institute, Cairo, Egypt, Postal Code: 12622 (corresponding author to provide fax: +20-2-33351631, e-mail : maamoun@eri.sci.eg).

Y. M. Alsayed is with the Electronics Research Institute, Cairo, Egypt.

A. Shaltout is with the Faculty of Engineering, Cairo University, Cairo, Egypt.

terminals. If the inverter operation starts by state (100) to be state 1, it is possible to compute the voltage space vectors for all inverter states which are shown in the complex space vector

plane in Fig.2 [3]. The six active voltage space vectors are of equal magnitude $(2/3) V_{dc}$ and mutually phase displaced by 60° , as shown in Fig. 3. The peak fundamental phase voltage that may be produced by the inverter for a given dc link voltage occurs under six-step operation, and is given by :

$$V_{1,six-step} = \frac{2}{\pi} V_{dc} \quad (1)$$

On the other hand, the maximum achievable peak fundamental phase voltage for conventional sinusoidal modulation as shown in Fig. 3 is:

$$V_{1,sin-pwm} = \frac{V_{dc}}{2} \quad (2)$$

From equations (1) and (2), only 78.5% of the inverter capacity is used.

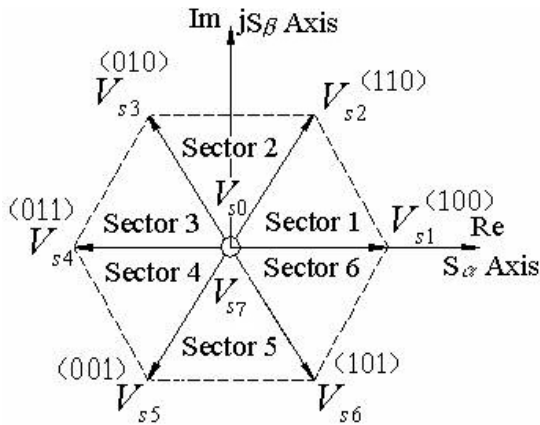


Fig. 2 Voltage space vectors for a three-phase VSI

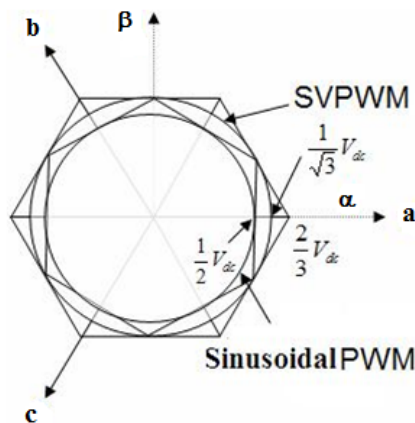


Fig. 3 Locus comparison of maximum peak voltage in sinusoidal PWM and SVPWM

The modulation index M of the reference voltage space vector V_s^* is defined as the ratio of the desired peak fundamental phase voltage to half the dc link voltage (maximum achievable peak fundamental phase voltage for conventional sinusoidal PWM) as the following:

$$M = \frac{V_1}{(V_{dc}/2)} \quad (3)$$

The largest possible peak phase voltage that may be achieved using the space vector modulation strategy corresponds to the radius of the largest circle that can be inscribed within the hexagon of Fig.3. Thus, the peak fundamental phase voltage that may be achieved is:

$$V_{1,svpwm} = \frac{V_{dc}}{\sqrt{3}} \quad (4)$$

which corresponds to a maximum modulation index $M_{max} \approx 1.15$. From equations (1) and (4), about 90.6% of the inverter capacity is used. This represents 15% increase in maximum voltage compared with the conventional sinusoidal modulation.

Consider the example depicted in Fig.4, in which the desired voltage is found to lie in Sector 1. Although, the inverter can not produce the desired voltage directly. It is possible to decompose it into two vectors, V_x and V_y , that lie on the two active inverter vectors on either side of the reference vector[2], [3], [9]. Therefore, in space vector notation:

$$V_s^* = V_x + V_y \quad (5)$$

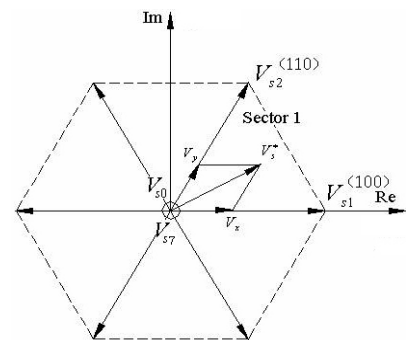


Fig. 4 Synthesis of desired space- vector voltage using realizable voltage vectors

where the vectors, V_x and V_y , are obtained by operating at the relevant inverter states, V_{s1} and V_{s2} , for suitable portions of the switching period, T_s . In general, when operating in

sector m , the reference vector may be decomposed according to :

$$V_s^* = \frac{T_m}{T_s} V_{s,m} + \frac{T_{m+1}}{T_s} V_{s,m+1} \quad (6)$$

where T_m and T_{m+1} are the times spent at adjacent active inverter states, $V_{s,m}$ and $V_{s,m+1}$. The remainder of the switching cycle is subdivided between the zero states :

$$T_{zero} = T_0 + T_7 = T_s - T_m - T_{m+1} \quad (7)$$

Having computed the active and zero state times for a particular modulation cycle, it is possible to produce the switching signals, PWM1, PWM2, and PWM3 to be applied to the inverter. The total zero time is most often divided equally between the two zero states. It is possible to satisfy the above restrictions by the use of symmetrical pulses as shown in Fig. 5 [8], [9]. The cycle begins in state 0, (000), with each inverter pole being successively toggled until state 7, (111), is obtained. The pattern is then reversed in order to complete the modulation cycle.

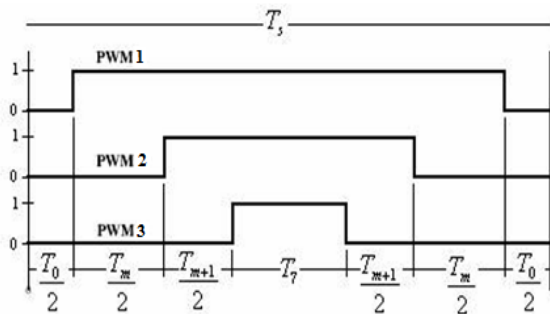


Fig. 5 Inverter switching signals for SVM in sector 1

III. MODEL OF PMSM

The stators of the PMSM and the wound rotor synchronous motor (SM) are similar and there is no difference between the back EMF produced by a permanent magnet and that back EMF produced by an excited coil. Hence the mathematical model of a PMSM is similar to that of the wound rotor SM [6], [7].

The stator d , q equations of the PMSM in the rotor reference frame are :

$$v_q = r i_q + P \omega_r \lambda_d + p \lambda_q \quad (8)$$

$$v_d = r i_d - P \omega_r \lambda_q + p \lambda_d \quad (9)$$

where

$$\lambda_q = L_q i_q \quad (10)$$

$$\lambda_d = L_d i_d + \lambda_m \quad (11)$$

where P is the pole pairs, p is the d/dt operator, v_q and v_d are the q , d axis voltages, i_q and i_d are the q , d axis stator currents, L_q and L_d are the q , d axis inductances, λ_q and λ_d are the q , d axis stator flux linkages, while r and ω_r are the stator resistance and rotor speed, respectively. λ_m is the flux linkage due to the rotor magnets linking the stator.

The electromechanical torque developed by the motor is :

$$T_{em} = \frac{3}{2} P (\lambda_d i_q - \lambda_q i_d) \quad (12)$$

by substituting equations (10), and (11) in equation (12),

$$T_{em} = \frac{3}{2} P (\lambda_m i_q + (L_d - L_q) i_q i_d) \quad (13)$$

The relationship between the electromechanical torque and the load torque is given as :

$$\frac{d\omega_r}{dt} = \frac{1}{J_m} (T_{em} - T_l - B_m \omega_r) \quad (14)$$

$$\frac{d\theta_r}{dt} = \omega_r \quad (15)$$

where B_m is the friction coefficient, T_l is the load torque and J_m is the moment of inertia. The inverter frequency is related to the rotor speed as the following :

$$\omega_e = P \omega_r \quad (16)$$

For dynamic simulation, the equations of PMSM presented in (8)-(16) must be expressed in state-space form as the following :

$$p i_q = \frac{1}{L_q} (v_q - r i_q - P \omega_r L_d i_d - P \omega_r \lambda_m) \quad (17)$$

$$p i_d = \frac{1}{L_d} (v_d - r i_d + P \omega_r L_q i_q) \quad (18)$$

$$p \omega_r = \frac{1}{J_m} (T_{em} - T_l - B_m \omega_r) \quad (19)$$

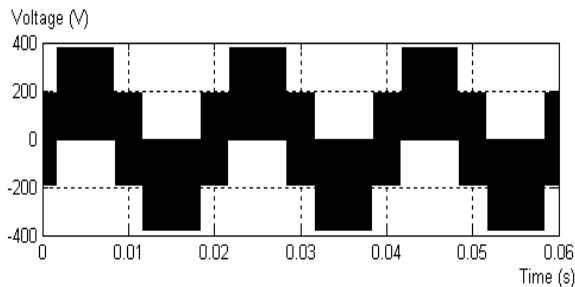
IV. SVPWM INVERTER FEEDING A PMSM

The SVPWM technique is used to produce the switching control signals to be applied to the three-phase inverter circuit given in Fig. 1. The SVPWM inverter is used to offer 15% increase in the dc link voltage utilization and low output harmonic distortions compared with the conventional sinusoidal PWM inverter. The control strategy of the SVPWM inverter is the voltage/frequency control method, which is based on the space-vector modulation technique. For constant

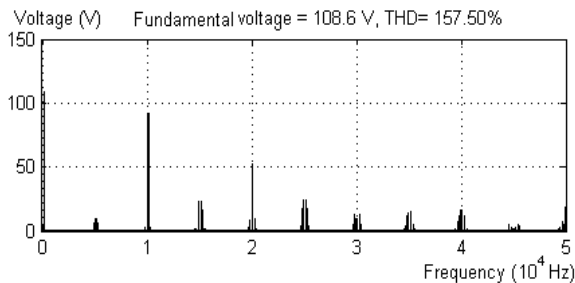
torque output, the air gap flux in the motor is maintained constant by operating on a constant voltage/frequency supply. However, the analysis above assumes negligible winding resistance, whereas, in practice, at low frequencies the resistive voltage drop becomes significant compared with the induced voltage. This voltage drop causes a reduction in the air gap flux and motor torque. In order to maintain the low-speed torque, the voltage/frequency ratio must be increased at low frequencies. The SVPWM-PMSM drive is a part of a PMSM drive system controlled by using conventional PI controller.

V. SIMULATION RESULTS

The SVPWM inverter which feeding a three-phase PMSM is simulated using the Matlab software package. The simulation is performed under the following conditions : $V_{dc}=570$ V, switching frequency=5 kHz, and three-phase PMSM (0.95 kW, 3 N.m, 400 V, 2.7 A, 150 Hz, 3000 rpm, $r=3.15 \Omega$, $L=17.5$ mH, voltage constant = 97 mV.min, $J=0.00031$ kg.m², and $P=3$). Figures 6 and 7 show the motor phase voltage and motor line voltage at inverter frequency $f_o=50$ Hz and modulation index $M=0.38$. Figures 8 and 9 show the reference input voltage vector and the actual output voltage vector in the (α - β) planes. Also, the motor current at different loading conditions is shown in Figures 10 and 11. Thus, the motor current has low harmonic distortion. The speed response of the motor drive system is shown in Fig. 12.

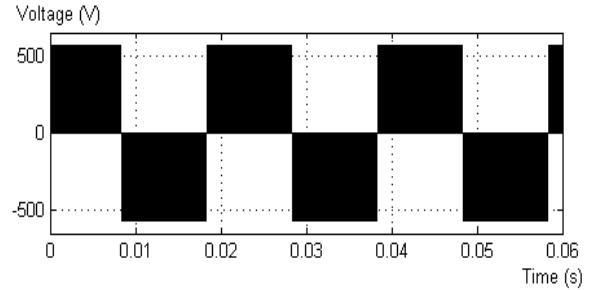


(a)

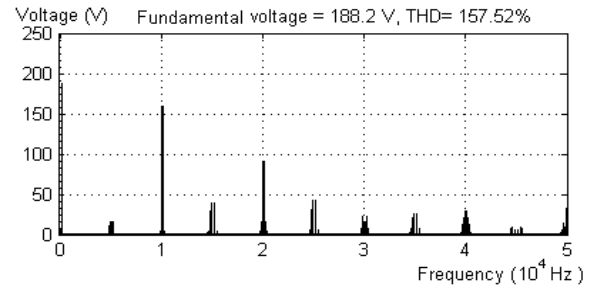


(b)

Fig. 6 Phase voltage of the motor at $f_o=50$ Hz and $M=0.38$
 (a) voltage waveform
 (b) voltage spectrum (peak value) and THD



(a)



(b)

Fig.7 Line voltage of the motor at $f_o=50$ Hz and $M=0.38$
 (a) voltage waveform
 (b) voltage spectrum (peak value) and THD

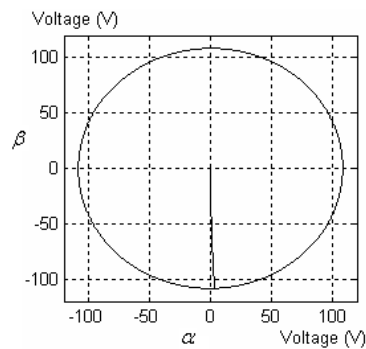


Fig. 8 Locus of reference input voltage vector in the ($\alpha - \beta$) plane

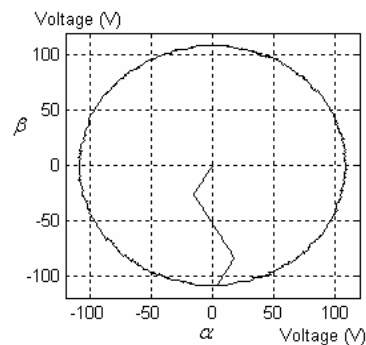
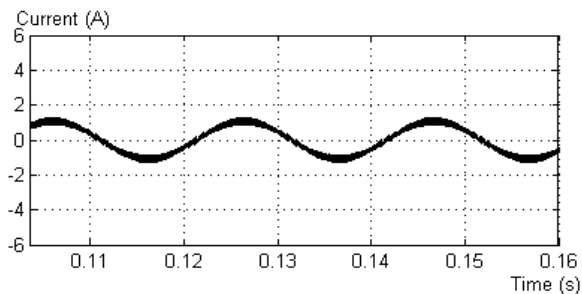
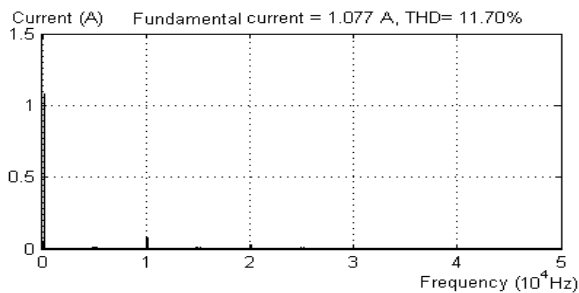


Fig. 9 Locus of actual output voltage vector in the ($\alpha - \beta$) plane



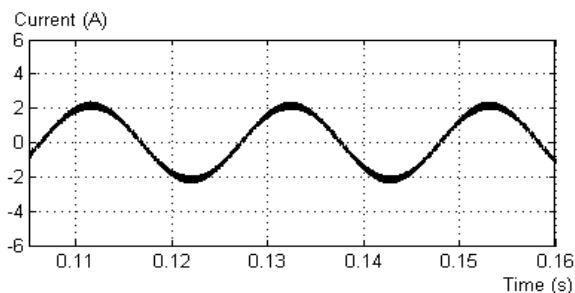
(a)



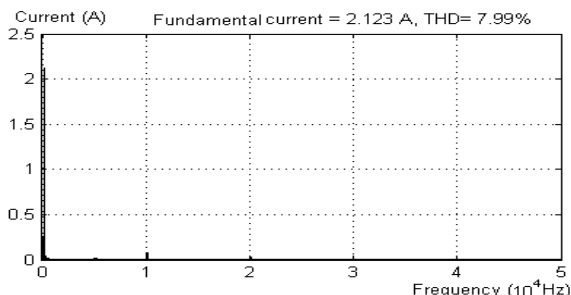
(b)

Fig. 10 Current of the motor at $f_0=50$ Hz, $M=0.38$, and $T=1.5$ N.m

(a) current waveform
 (b) current spectrum (peak value) and THD



(a)



(b)

Fig. 11 Current of the motor at $f_0=50$ Hz, $M=0.38$, and $T=3$ N.m

(a) current waveform
 (b) current spectrum (peak value) and THD

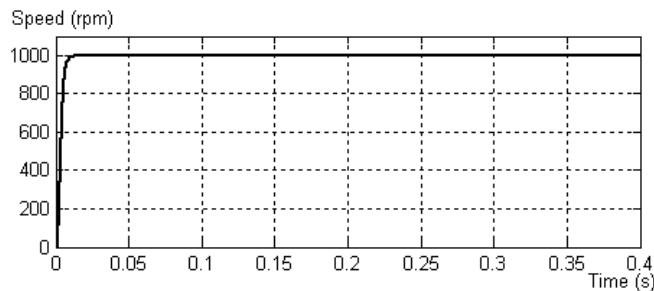


Fig. 12 Speed response of the motor drive system at load $T=3$ N.m

VI. CONCLUSION

In this paper, a SVPWM-PMSM drive has been introduced. The SVPWM inverter is used to offer 15% increase in the output voltage and low output harmonic distortions compared with the conventional sinusoidal PWM inverter. The control strategy of the SVPWM inverter is the voltage/frequency control method which is based on the space-vector modulation technique for constant torque operation. The advantages of the proposed drive are confirmed by the simulation results.

REFERENCES

- [1] R. Arulmozhiyal, and K. Baskaran, "Space vector pulse width modulation based speed control of induction motor using fuzzy PI controller," *International Journal of Computer and Electrical Engineering*, vol. 1, no. 1, April 2009, pp. 98-103.
- [2] Z. Wang, J. Jin, Y. Guo, and J. Zhu, "SVPWM techniques and applications in HTS PMSM machines control," *Journal of Electronic Science and Technology of China*, vol. 6, no. 2, June 2008, pp. 191-197.
- [3] A. Maamoun, A. Soliman, and A. M. Kheirelden, "Space-vector PWM inverter feeding a small induction motor," in *Proc. IEEE Int. Conf. on Mechatronics*, Komamoto, Japan, May 2007, pp. 1-4.
- [4] W. Kaewjinda, and M. Konghirun, "Vector control drive of permanent magnet synchronous motor using resolver sensor," *ECTI Trans. Electrical Eng., Electronics, and Communications*, Thailand, vol. 5, no. 1, Feb. 2007, pp. 134-138.
- [5] M. Štulrajter, V. Hrabovcová, and M. Franko, "Permanent magnets synchronous motor control theory," *Journal of Electrical Engineering*, Slovak Republic, vol. 58, no. 2, 2007, pp. 79-84.
- [6] P. Pillay, and R. Krishnan, "Modeling, simulation, and analysis of permanent-magnet motor drives, part I: the permanent-magnet synchronous motor drive," *IEEE Trans. Industry Applications*, vol. 25, no. 2, March/April. 1989, pp. 265-273.
- [7] P. Pillay, and R. Krishnan, "Modeling of permanent magnet motor drives," *IEEE Trans. Industrial Electronics*, vol. 35, no. 4, Nov. 1988, pp. 537-541.
- [8] W. Zhang, and Y. Yu, "Comparison of three SVPWM strategies," *Journal of Electronic Science and Technology of China*, vol. 5, no.3, Sept. 2007, pp. 283-387.
- [9] A. Saadoun, A. Yousfi, and Y. Amirat, "Modeling and simulation of DSP controlled SVPWM three - phase VSI," *Journal of Applied Sciences*, vol. 7, no. 7, 2007, pp. 989-994.